

Supplementary Information

Understanding the temperature-dependent evolution of solution processed metal oxide transistor characteristics based on molecular precursor derived amorphous indium zinc oxide

Shawn Sanctis,^a Rudolf Hoffmann,^a Ruben Precht,^b

Wolfgang Anwand^c and Jörg J. Schneider^{a*}

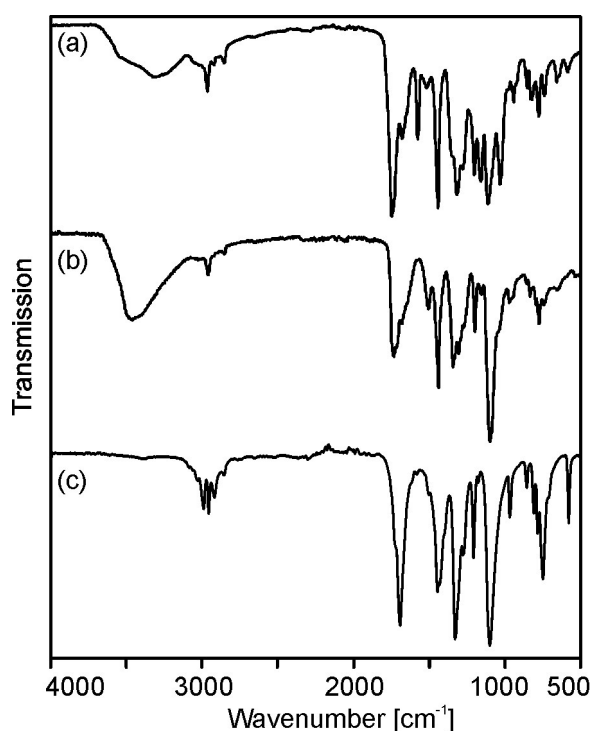


Figure S1: IR spectra of (a) dimethyl-2-nitromalonate¹⁶, (b) [Zn₃(OH)₄(dmm-NO₂)₂]¹⁶ and (c) [In₃O₃(dmm-NO₂)₃]²·toluene (**2**).

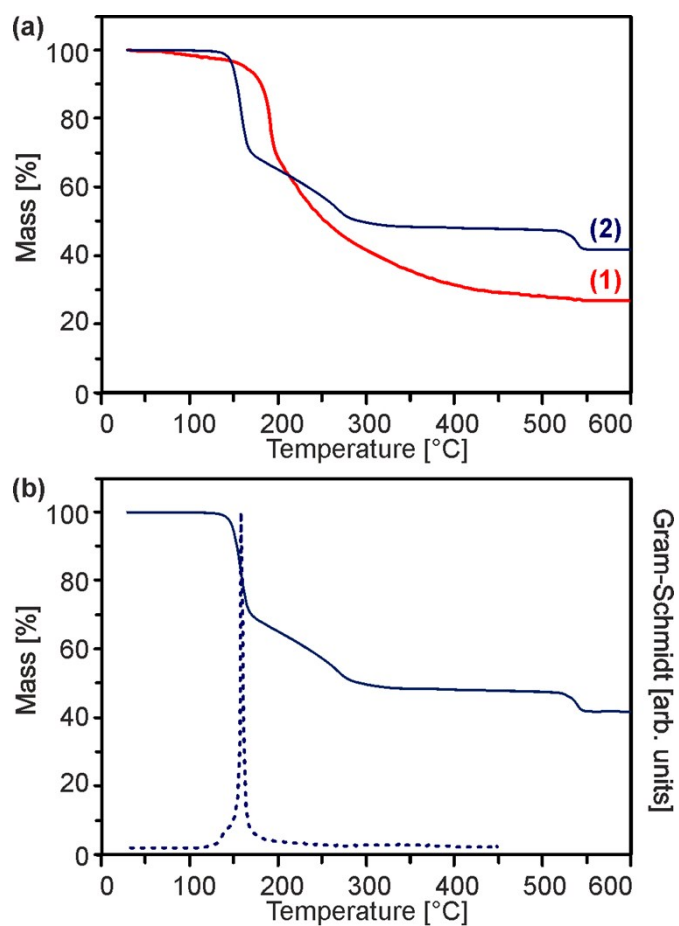


Figure S2: (a) Thermogravimetric mass loss curves of $[\text{Zn}_4\text{O}(\text{dmm-NO})_6]$ (**1**) and $\text{In}_3\text{O}_3(\text{dmm-NO}_2)_3$ (**2**) in oxygen. (b) Thermogravimetric mass loss curve (straight line) and corresponding Gram-Schmidt signal (dotted line) of (**2**).

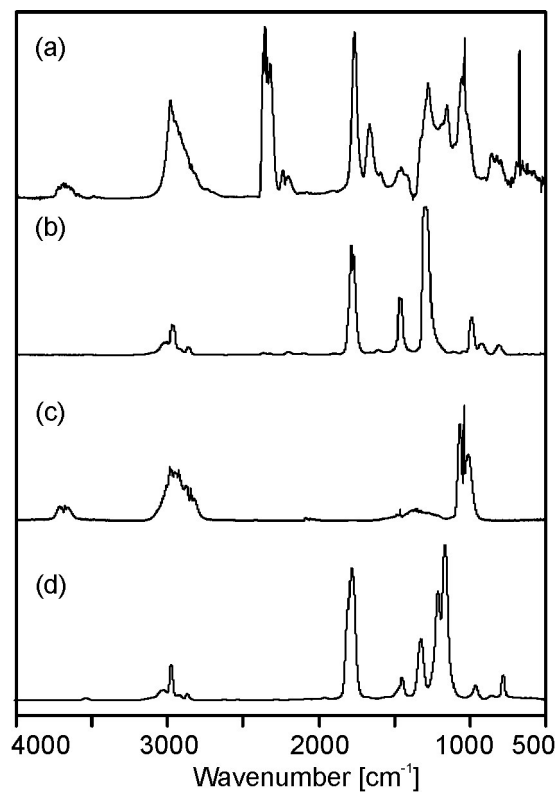


Figure S3: (a) Gas phase IR spectrum corresponding to the maximum of the Gram–Schmidt signal in Figure S1(b) from the decomposition of $\text{In}_3\text{O}_3(\text{dmm-NO}_2)_3(\mathbf{2})$ as well as reference spectra of (b) dimethyl carbonate, (c) methanol and (d) dimethyl oxalate.

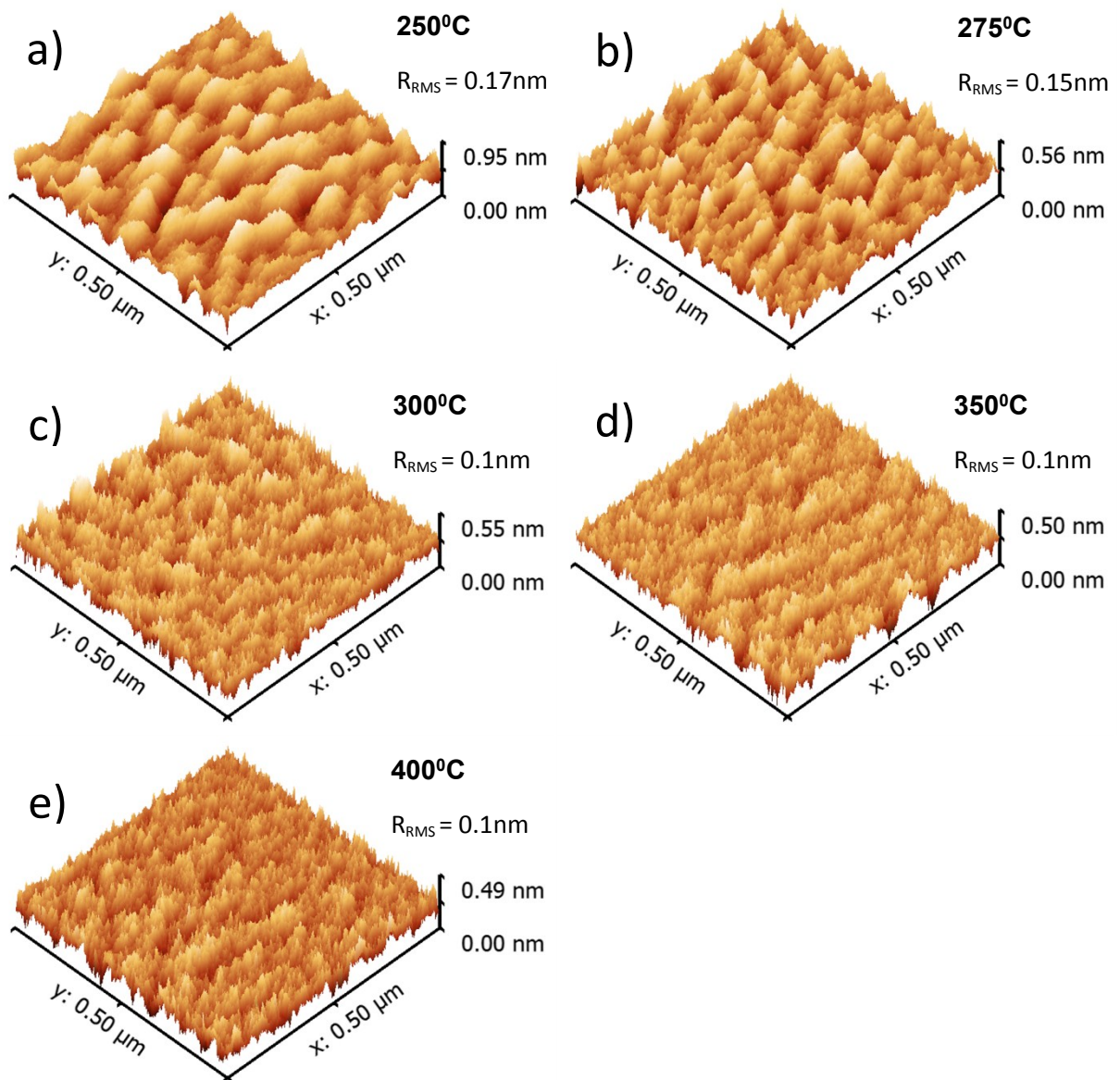


Figure S4: AFM micrographs and the obtained root mean square roughness (R_{RMS}) for the IZO films annealed at increasing temperatures from 250 to 400°C.

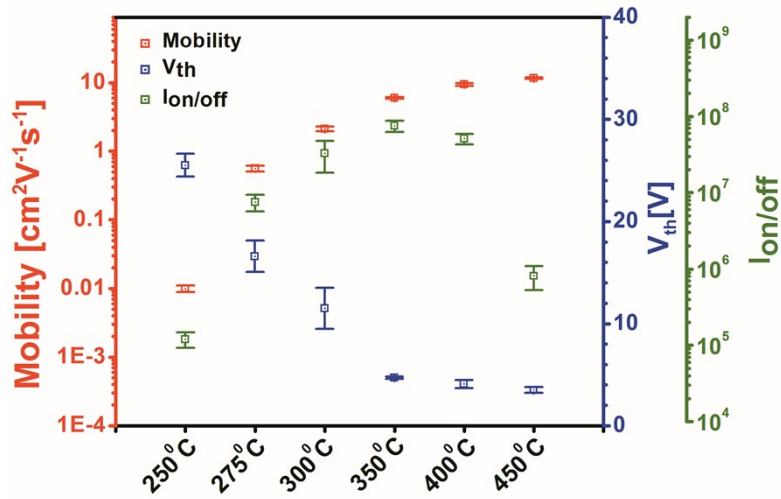


Figure S5: Averaged saturation field-effect mobility (μ_{SAT}), threshold voltage (V_{th}) and current on-off ratio ($I_{on/off}$) of eight devices with the corresponding standard deviations for the IZO TFTs annealed at increasing temperatures from 250 to 450°C.

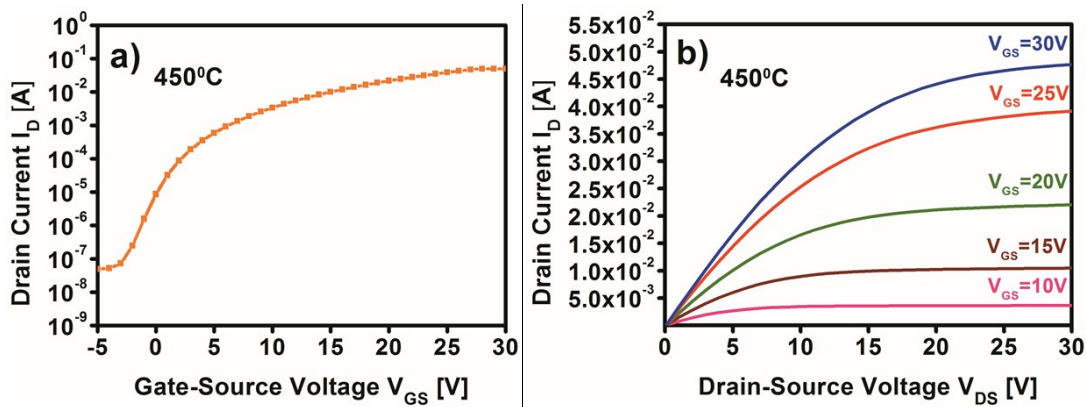


Figure S6: a) Transfer characteristics and b) Output characteristics of the TFT device for IZO films annealed at 450 °C.